Development of Thermal analysis, Hardness and tensile testing of Friction Plug Welding

Vishan Singh, M.Tech Scholar, Department of Mechanical Engineering, Goel Institute of Technology & Management, Lucknow, India.
Shiv Kumar, Assistant Professor, Department of Mechanical Engineering, Goel Institute of Technology & Management, Lucknow, India.

Abstract— When two dissimilar or similar materials are joined using friction plug welding (FPW), there is no need for external heat or for the materials to be in their molten condition. Friction welding is more of a forgery than a genuine fusion welding procedure because no melting occurs during the operation. It is possible to increase the efficiency of joints by interpolating heat sources or preheating the work piece surface. When determining the generation of heat flux at the mean surface, the friction coefficient must be taken into consideration as well. The breadth of the land can be changed by varying the diameter of the plug and observing how this affects the temperature distribution. It is possible to calculate the influence of pre-heating by applying mathematical and analytical models. When different plug diameters and pre-heating temperatures were used, the temperature distribution values throughout the work piece were calculated for temperatures ranging from 2500C to 5500C.
The effects of temperature history controls on joint microstructures, hardness distributions, and tensile qualities were investigated.
Using a non-consumable tool, frictional heat is generated between the abutting surfaces during the procedure. Among other things, welding features such tool rotational speed, welding speed, axial force, and tool pin profile, among other things, have a considerable impact on the determination of joint strength. An attempt was made to develop an empirical link between FPW parameters in order to estimate the tensile strength of friction plug welding.

Keywords— Friction plug welding, Heat, Friction, Temperature, Tensile strength, Tool pin profile, welding speed.

I. INTRODUCTION

Friction welding is one of these machining procedures in which heat is generated between the two pieces that are being welded as a result of friction between them. This technology is now being employed in companies all over the world as a dependable and automated welding procedure.
In the joining process of friction welding, materials are adjusted under compressive force contact of workpieces that are rotating relative to each other to generate heat and plastically displace material from rubbing down surfaces that do not melt. [6-8] The use of filter metal and flux is not required with this technique.
Friction Stir welding, a solid-state method, is being used to join aluminium alloys of various types that have previously been difficult to weld together. Distortion is reduced and welding is free of porousness as a result of the re-solidification and non-melting of the metal. A non-damperable, rotating tool is used to keep the plates to be welded in contact with the surface. Heat is generated by tool movement in the direction of the welding surface, which is less than the solidus temperature; the welding joints are built up as a result. When the shoulder comes into contact with the surface of the plates, the temperature rises as a result of the heat generated, and the pin of the shoulder stirs up the joining surface, allowing the material on the backside of the pin to flow through the joint. The metal cools as the tool passes through it, resulting in the formation of a processed zone. It is necessary to employ a tool made of a harder material than the plates that are to be connected. As harder tools are being produced, the FSW technique is being used to combine materials that are subjected to high temperatures at the moment [9-11].
Friction plug welding (FWP) is a type of welding in which originally incorrect weld material is changed by plugging it back into its original position, which is accomplished through friction welding.
The basic principle is illustrated in figure 1.

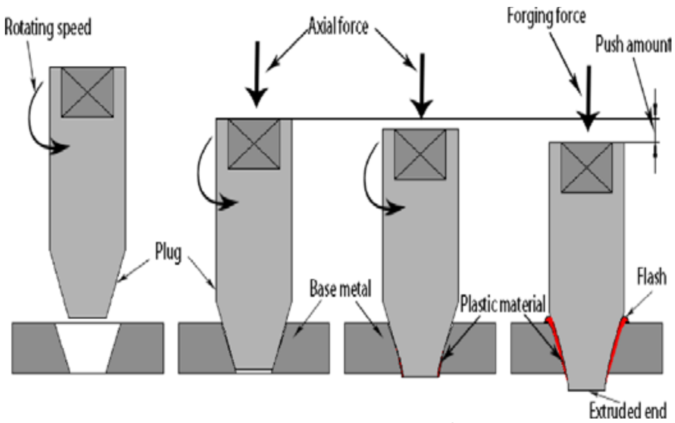

Figure 1: Schematic diagram of FPW process

The FPW key procedure is as follows: first and foremost, a hole is created at the stand where the hole is to be generated with the necessary geometrical specifications. Second, an expeditiously rotating plug is inserted into a hole under the operation of an axial force, resulting in rapid frictional heating and defacement at the interface between the hole and the plug, which is most likely referred to as the welding phase. Next, the plug rotation is suddenly stopped and a moulding force is applied to the weld surface, resulting in an FPW weld being formed when the hole is filled, as shown in the illustration. Remove the plug and quern the surface plain [12-13] at the end of the procedure.

The friction stir welding (FPW) process is used for correcting weld flaws in the presence of friction (FSW). When compared to other welding technologies, the FPW performs significantly better when fusing aluminium alloys together. It is possible to correct the deficiency by increasing joint strength, reducing stress, and decreasing distortion. An example of friction plug welding (FPW) is when a rounded plug is spun in the hole while a force is applied to ensure that the hole is filled.

It has been suggested that the use of a friction plug welding technique can be utilized to correct any faults that may develop during the friction stir welding process. This is one of the recommended methods for doing so. In Figure 2, you can see a schematic representation of the friction plug weld process.

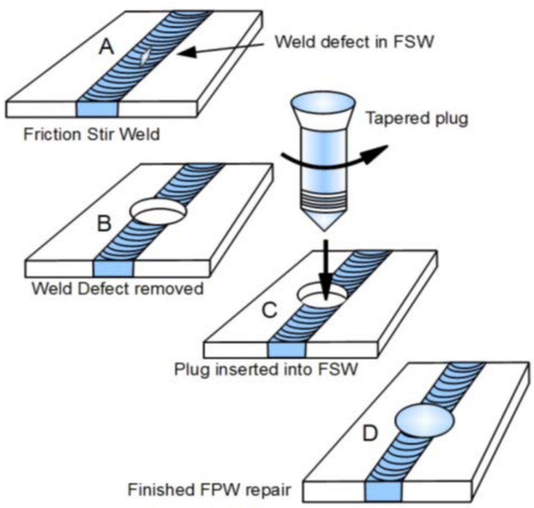

Figure 2: Friction plug weld process

The joining process begins when the moving part generates frictional heat at the bottom half of the hole, allowing plasticization to take place at that location. The 3-D finite element analysis of aluminium FSW was carried out in order to examine the heat transmission and thermal phenomena of the material. Two welds, one with a very short pin and one with a lengthy pin, were examined. The boundary condition for FSW has been defined, and the heat flow has been determined [24-26].

Friction plug welding of aluminium alloy is discussed in this paper in order to develop a mathematical model of the process. It is possible to calculate the generation of heat flux on the basis of frictional heat. The pre-heating of the material is varied in different ranges in order to determine the impact on the temperature profile in the work piece. By utilizing one-dimensional heat conduction, it is possible to calculate the temperature distribution for varied plug diameters.

II. Literature Review

Friction stir welding (FSW) is newly introduced process which provides better quality joints and also low cost. For any type of research work in this area, the most important phase is to get knowledge of already available literature.

Kwon and colleagues [1] reported on friction stir welding between 5052 aluminium plates with a thickness of 2 mm in a friction stir welding experiment. The rotational speed of the tool can be varied from 500 to 3000 rpm, with a constant stride speed of 100 mm/min throughout. The rotational speed of the tool for welded joints ranged from 1000 to 3000 rpm. At [500, 1000, and 2000 rpm, an onion ring structure was seen in the friction-stir-welded zone (SZ) of the friction-stir-welded process. On onion rings, it was discovered that the tool rotation speed (TRS) had an effect. The gain size in the SZ is less than that in base metal, and it decreases as the TRS is reduced. The results of the experiment revealed that the tensile strength, or joint strength, is greater than the parent metal. In addition, the joint's ductility was determined to be no greater than that of the base alloy.

It was the goal of the study directed by G. CAO and S. KOU [2] to see if the boundary temperature in the work piece could cause liquation during friction stir welding (FSW) of aluminium alloys and limit the lower bound of the melting temperature range, as had been observed in some computer simulations. The work piece material, AA 2219, an aluminum-copper alloy, was chosen because it falls inside a specific lower bound of the melting temperature array and has a eutectic temperature of 548 degrees Celsius. FSW of Alloy 2219 was introduced in addition to gas metal arc welding (GMAW) of Alloy 2219 in order to provide a stratum for checking liquation in friction stir welding (FSW) of Alloy 2219. The results of the investigation using both scanning electron microscopy and optical microscopy revealed that in GMAW of Alloy 2219, q (Al2Cu) particles featured as in-situ micro sensors, which shows liquation due to reaction between Al and Cu forms eutectic particles when the temperature reaches eutectic temperature. In FSW, no evidence of q-induced liquation was discovered, indicating that the eutectic temperature was not reached throughout the experiment.

According to J. Adamowski et al. [3, they investigated microstructural changes and mechanical qualities in FSW produced by AA 6082-T6 with varying process settings. The tensile testing of the welds was done, and the relationship between the process factors was examined. The microstructure of the weld contact was studied using an optical microscope. In addition, the micro hardness of the resultant joint was assessed.

Hardness loss was found in the weld nugget and the heat affected zone (HAZ), and test welds demonstrated increased resistance as the welding speed was increased under observation. The temperature asymmetry and kinetics of the friction stir welding process were the underlying causes of this phenomenon. The initial stage of longitudinal, volumetric defect was discovered at the interface of the weld nugget and the TMAZ. The hardness of the material was lower than that of fusion welding (FW). The presence of worm hole (tunnel) flaws was discovered in the nugget zone.

H.J.LIU and colleagues [4] investigated the friction welding characteristics of AA 2017-T351 sheet, in which they investigated the microstructure of the weld joints and discovered a relationship between the parameters. The relationship between revolutionary strength and pitch,Vickers, was depicted on graphs. The hardness and distance from the weld centre, the placement of fractures at the joints, and the revolutionary pitch are all factors to consider. According to the results of the tension tests and the hardness tests, FSW also has the effect of decreasing the tensile strength of the material and softening the material. In accordance with the microscopic investigation, successive generations of cracks in the joint at the interface between the thermodynamically impacted zone and the weld nugget are observed.

M.Vural et al. [5] investigated the FSW competency of the aluminium alloys EN AW 2024-0 and EN AW 5754-H22 in the laboratory. These aluminium alloys are widely employed in a variety of industrial applications. The results of the experiment revealed that the hardness value of EN AW 2024-0 at the weld area has risen by approximately 10 to 40 Hv. This could be the result of the creation of a compact grain structure and the subsequent recrystallization. However, the hardness of EN AW 5754-H22 reduced as a result of the creation of loose grain structure and recrystallization. The welding performance of EN AW 5754-H22 is 57 percent, while the welding performance of EN AW 2024-0 is 96.6 percent. The weldability of different aluminium alloys, such as EN AW 2024-0 and EN AW 5754-H22, has been demonstrated to be 66.39 percent. In the investigation of the welding zone, the scanning electron microscope revealed that there was no change in the microstructure in the welding zone. The hardness distribution did not demonstrate any significant changes in hardness at the weld zones.

III. Mathematical Modeling

FPW modeling can be done in many steps. The friction pressure and heat generation across the interface are considered uniform. Some assumptions are incorporated in model:

- The co-efficient of friction is constant and heat is generated only by friction.
- The behavior of work pieces material has assumed perfect elastic-plastic.
- The heat loss due to radiation has been ignored, as plasticity was assumed.

Temperature distribution

Generation of Heat

The thermal modeling equation for friction welding procedure, is mentioned as eq. (1)

$$\mathrm{K}\left[\frac{\partial^2 \mathrm{T}}{\partial \mathrm{x}^2}+\frac{\partial^2 \mathrm{T}}{\partial \mathrm{y}^2}+\frac{\partial^2 \mathrm{T}}{\partial \mathrm{z}^2}\right]+\mathrm{G}=\rho \mathrm{c}\frac{\partial \mathrm{T}}{\partial \mathrm{t}}$$

$$K\left[\frac{\partial^2 T}{\partial x^2}+\frac{\partial^2 T}{\partial y^2}+\frac{\partial^2 T}{\partial z^2}\right]+G=\rho c\frac{\partial T}{\partial t} \qquad (1)$$

ρ, c and K are temperature dependent, Friction welding process contains the heat generation by friction between two work pieces qf, and heating from irreversible plastic deformation of both work pieces qp [14-16]. Heat generation rate G is given as,

$$G=q_f+q_p \qquad (2)$$

In this study, it has been assumed that Friction law of Coulomb is followed for friction between work pieces; Generation of heat due to plastic deformation (qp) and due to friction (qf) and can be determined by equations 3 & 4,

$$q_f=2\pi RN\mu F_n \qquad (3)$$

$$\eta\sigma\varepsilon \qquad (4)$$

For heat flux generation, the correlation between torque and heat energy is to be made. Heat production and the change of heat may be calculated by dimensions of parts and operating characteristics. By using machine torque, heat generation of friction can be calculated as below [27],

$$qf=\left(\frac{2\pi N\zeta}{60A}\right)*\eta \qquad (5)$$

Heat generation can also be determined using equation no 6,

$$q=U*A*\Delta T=U*A*(T_{in}-T_{amp}) \qquad (6)$$

Distance from contact surface (T_L) is calculated by

$$\frac{T_L-T_\alpha}{T_b-T_\alpha}={}^{1}/_{\cosh(mL)} \qquad (7)$$

Where, At the nominal distance the temperature is T_L,T is denoted as ambient temperature and Tb is temperature of base plate. Tb can be determined by,

$$T_b=T_p+T_f \qquad (8)$$

Where, Tp is defined as the Pre-heat temperature and Tf is temperature due to friction, produced by generation of heat

$$m=\sqrt{\frac{hp}{KA}} \qquad (9)$$

Temperature at distant place from contact surface is determined,

$$\frac{T-T_\alpha}{T_b-T_\alpha}=e^{-mx} \qquad (10)$$

Where,
T is denoted as temperature distribution,

$T\alpha$ = ambient temperature,
T_b = base plate temperature,
x = distance of contact surface.
On the basis of heat conduction (HC) equations, as explained above, heat flux can be determined. The variation of temperature distribution can be studied by varying the temperature, preheating, and distance of work piece and contact area. The plug diameter is depends upon land width.

Hardness distribution

With the Hardness tests, the measurement of resistance of material to indentation is done. Strength of the material is indicated by its hardness. In the test, indenter made of harder material than test material, is pressed with force on the surface of tested material. After that, the indentation is determined.Hardness of material is inversely proportional to the indentation area. There is different-different types of hardness tests in which Rockewell, Brinell and Vickers are the common tests.Vickers tests were used to study the hardness of both the welds and base material in the course of this work . A diamond pyramid indenter is used by Vickers hardness test, which produces a pyramidal indentation [28].

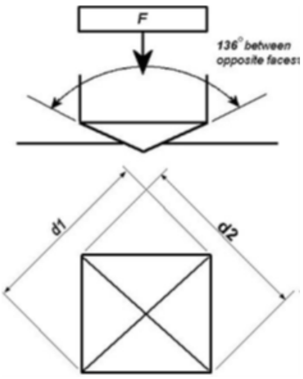

Figure 3: Vickers Hardness Test

The hardness is determined after the measurement of indentation:

$$VHN = 1.72 * \frac{F}{d1*d2} \tag{11}$$

Where 'VHN' is denoted as Vickers Hardness Number, 'F' is force of indentation and d1, d2 are the distances of opposite corners of the indentation [29].
In Vickers hardness test method indenter is of diamond which indents the test material, in the form of a right pyramid with angle of 136 degrees between two opposite face subordinated a load of 1- 100 kgf and a square base. For 10-15 seconds,full load is normally applied. The two diagonals of the indentation were remained in the surface of material on removal of the load are measured using a microscope and their average determined.Sloping surface area of the indentation is calculated. Vickers hardness is the quotient found after division of the kgf load by the square mm area of indentation. From calculation of force-area ratio using the area of diamond indents in the base material,the hardness number is determined. Three surfaces were tested for every material;the longitudinal surface,the transversal surface and the top surface. Clamping area of conventional bus bar ends is thinner and flattened than extruded part of bus bar.So, both the flattened and the extruded parts had their hardness investigated. A number of tests can be made for every sample and the indentations made so that they form a square as given in figure 3.

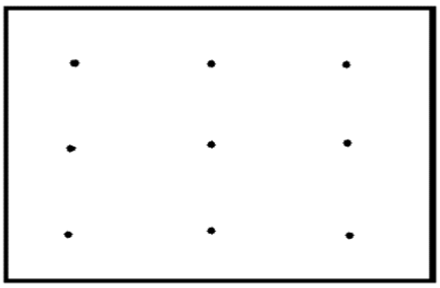

Figure 4: Hardness indentations for base materials

The hardness profile of FPW joint can be measured in three layers i.e. lower layer,upper layer and middle layer. The shape of the hardness profile would be in W-shape and the hardness of FPW joint is depends upon microstructure and phases in different zones.

The hardness distribution on aluminum joints (AA5A06) is varied slightly for all the welding parameters. The maximum hardness appeared near the NZ and TMAZ. The reason for this AA5A06 joints is non-heat treatable alloy, and therefore the temperature variation does not significantly affect the hardness. Near the NZ and TMAZ, the hardness was partially improved due to the refinement of the grains as a result of stirring action.

Tensile properties

Tensile strength is defined as the ability of a material to withstand loads that cause it to stretch. Tensile strength (TS) is the ability to withstand tension (being pulled apart), whereas compressive strength (CS) is the ability to withstand compression (being pushed together). The ultimate tensile strength (UTS) of a material is defined as the utmost amount of stress that it can withstand when being stretched or pulled before breaking or cracking. Brittle failure is a term used to describe a material that breaks very quickly without undergoing plastic deformation. Brittle failure can occur in a variety of materials. Other materials, particularly those that are highly ductile, such as the majority of metals, exhibit some plastic deformation and possibly necking before they shatter. A tensile test is typically used to determine UTS. The engineering stress versus strain curve is recorded during the test (S-S). The maximum point of the stress-strain (S-S)curve is designated as UTS. Since this feature is known as the intense property, the value of UTS does not depend on the size of the test specimen in this case as well. Additionally, it is dependent on other parameters, such as specimen preparation, the temperature of the test environment and material, and the presence or absence of surface imperfections on a specimen. In the design of ductile members, tensile strengths (TS) are not typically considered; nevertheless, they are important in the design of brittle elements [19]. Stress is the term used to describe the amount of force applied per unit area. Linear elastic behaviour is exhibited by many materials, and is described by a linear stress-strain relationship, as illustrated in figure 4. Generally speaking, the elastic nature of materials extends into a non-linear region, which is represented by the point at which deformations are perfectly recoverable upon removal of the load; this means that in tension, a specimen loaded elastically will elongate, but it will return to its original shape and size when the load is removed. Deformations of ductile materials, such as steel, occur entirely in the plastic zone above this elastic region. While a plastically deformed specimen does not perfectly regain its normal size and shape after being unloaded, it does so to a significant extent.

After yield, ductile metals go through a period of strain hardening, during which the value of stress increases again in proportion to the increase in strain, and they begin to neck as the cross-sectional area of the specimen shrinks as a result of plastic flow.

When necking becomes significant in a sufficiently ductile material, the engineering stress-strain (S-S) curve is reversed (figure 5); this is owing to the fact that the engineering stress is calculated using the original cross-sectional area before necking [20, 30] and the engineering stress is reversed. When the engineering S-S curve reaches its maximum stress, the reversal point is reached, and the engineering stress coordinate of this point is ultimate tensile strength (UTS), as indicated by point 1, the reversal point is reached.

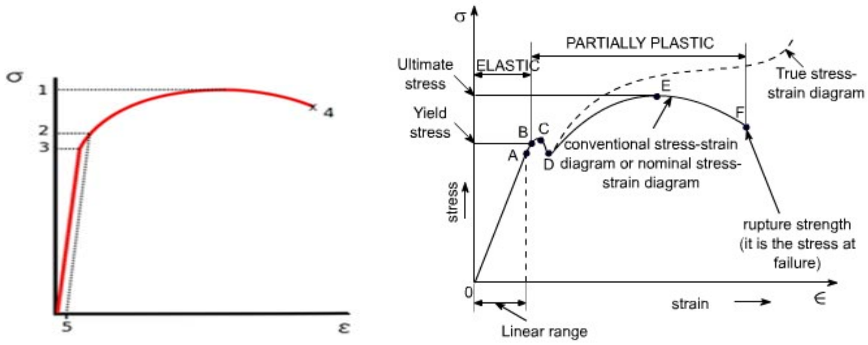

Figure 5: (a) & (b): Stress-Strain Curve

The points details of curve are given below,

1 → Indicate the Ultimate Tensile Strength (UTS)
2 →Yield Strength
3 →Proportional Limit Stress
4 →Fracture
5 →Offset Strain

Yield strength(σy) is point from where plastic deformation gets start. It is hard to specify correctly.But conventionally it is denoted as intersection of the curve with a parallel straight line to elastic part of the curve offset 0.2% on x-axis.The yield strength is also defined as the stress needed to deform material by 0.2% permanently.Slope of elastic part of the curve is known as modulus of elasticity, E. Tensile strength(TS) or

Ultimate tensile strength(UTS), is the maximum stress achieved during test. When material starts to reach that point, the fractured cross-sectional area experiences reduction. This is the reason why the original area of sample can't be used to model the true stress(σT) given below

$$\sigma T = \frac{P}{A\ actual} \quad (11)$$

For most of the metals approximation of the true stress is possible - true strain (ϵT) curve between yield stress(YS) and ultimate tensile stress(UTS) by equation shown below

$$\sigma T = K * \in_T^n \quad (12)$$

Where n and K are constant whose value change for every material.
From tensile test, ending value acquired is toughness of material. Toughness represents ductility and combination of strength and is the ability of material to bear mechanical energy up to failure point. Its value is equal to area contained under the stress-strain curve and numerically given as

$$U_T = \int_0^{\epsilon f} \sigma * d \in \quad (13)$$

Where ϵf strain upon failure and UT is toughness.
Tensile testing is used to calculate the maximum load (tensile strength), the material can withstand without failure. The load value or elongation value is the basis of tensile test.
The stress-strain graph and fracture position of FPW sample welded at different conditions can be determined. The maximum ultimate tensile strength (UTS) is contained by FPW joint and elongation of its value equivalent to that of base metal. There are many regions to find the minimum hardness and maximum hardness. The loss for welded joint ultimate tensile strength and elongation is considered as disintegration of precipitates and distribution of ingredient particles.

Developing Mathematical Model

The response function tensile strength (TS) of the joints is a function of tool profile (P), rotational speed (N), welding speed (S) and axial force (F), and it can be expressed as [21-22]

$$TS = \oint(P, N, S, F) \quad (14)$$

The second-order polynomial (regression) equation used to represent the response surface 'Y' is given by

$$Y = b_0 + \sum b_i x_i + \sum b_{ii} x_i^2 + \sum b_{ij} x_i x_j \quad (15)$$

and for four factors, the selected polynomial could be expressed as

$$TS = b_0 + b_1(P) + b_2(N) + b_3(S) + b_4(F) + b_{11}(P^2) + b_{22}(N^2)$$
$$+ b_{33}(S^2) + b_{44}(F^2) + b_{12}(PN) + b_{13}(PS) + b_{14}(PF) + b_{23}(NS)$$
$$+ b_{24}(NF) + b_{34}(SF) \quad (16)$$

Where b_0 is the average of all responses and b_1, b_2,…. b_{23} are coefficients which depend on interaction effects and respective main of the parameters.Values of the coefficients have been determined using the given below expressions (rf13)

$$b_0 = 0.142857 * \left(\sum Y\right) - 0.035714 * \sum\sum X_{ii} Y$$

$$b_i = 0.041667 * \left(\sum X_i Y\right)$$

$$b_{ii} = 0.03125 * \left(\sum X_{ii} Y\right) + 0{:}\,00372 * \sum\sum X_{ii} Y - 0.035714 * \left(\sum Y\right)$$

$$b_{ij} = 0.0625 * \left(\sum X_{ij} Y\right)$$

Every coefficient was tested at 95% confidence level (CL) for their significance by applying students t-test with the use of statistical software package (SPSS). After calculating the significant coefficients, the relations were formed only using these coefficients [23-24]. To predict tensile strength of FPW joints, last mathematical relationship is formed between the FPW variables, developed by statistical design of experiments procedure are given below:

$$TS = \begin{Bmatrix} 240.86 + 6.71(P) + 4.38(N) + 9.29(S) + 5.96(F) \\ -14.66(P^2) - 8.17(N^2) - 10.54(S^2) - 13.79(F^2) \\ -1.68(PS) - 1.44(PF) - 2.19(SF) \end{Bmatrix} MPa$$

<u>Advantages:-</u>

- Strength is high
- Having good mechanical properties
- Heat input is low
- Quick process time
- Low cast

IV. Simulation Results

The research, analysis, and modelling used in this work are all done in-house. I intend to acquire the MATLAB software and install it on my computer system. After reading numerous research articles on friction plug welding, I intend to put the entire system together in the MATLAB software environment. MATLAB models for heat production analysis, hardness distribution, and tensile strength will be created by me in this project. The various sorts of simulation results will be studied in order to put the FPW to the test.

Temperature distribution

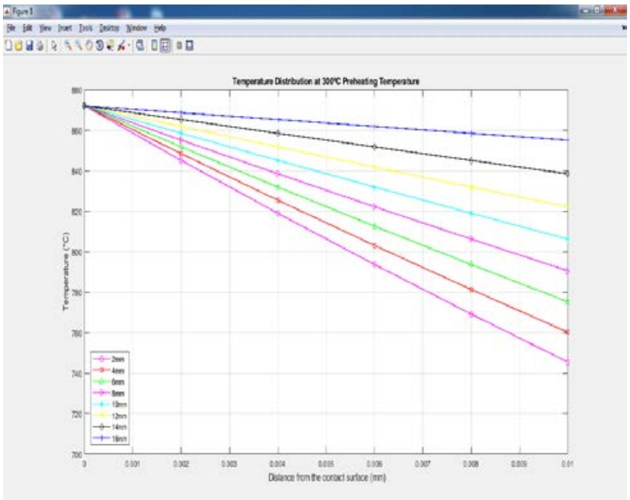

Figure 6: Temperature distribution at 300˚C preheating temperature

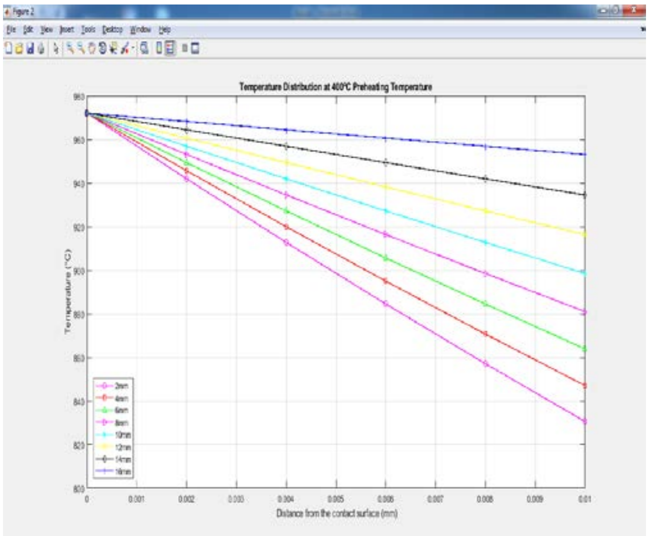

Figure 7: Temperature distribution at 400˚C preheating temperature

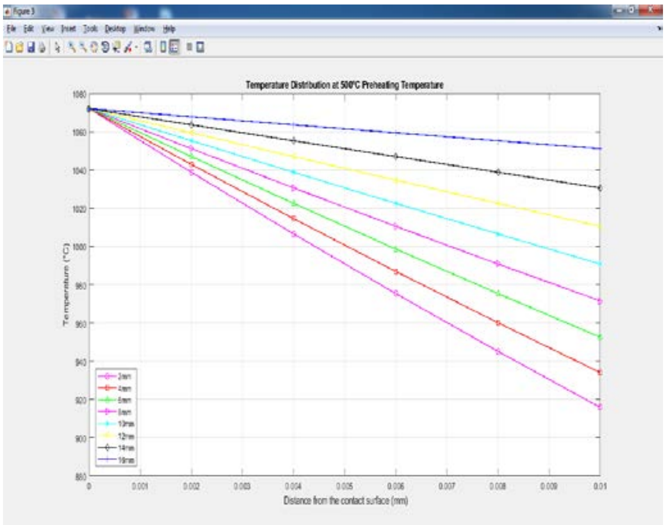

Figure 8: Temperature distribution at 500˚C preheating temperature

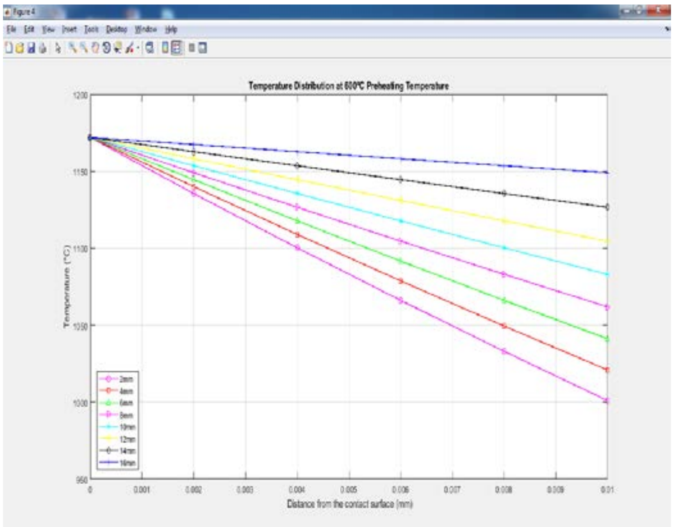

Figure 9: Temperature distribution at 600˚C preheating temperature

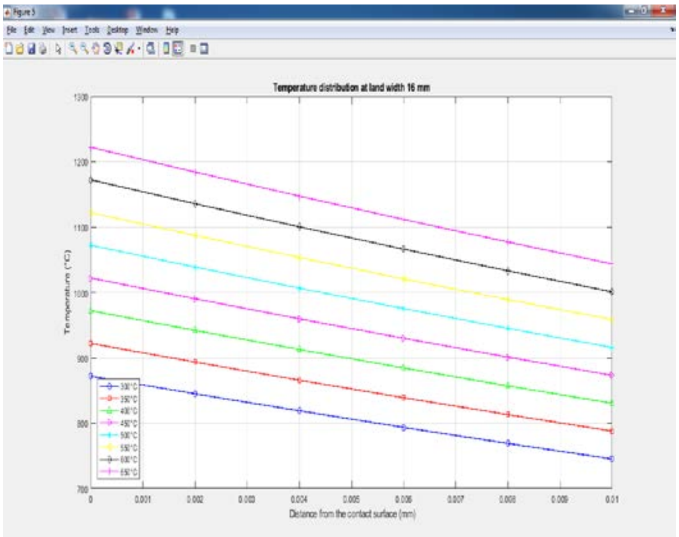

Figure 10: Temperature distribution at land width 16 mm

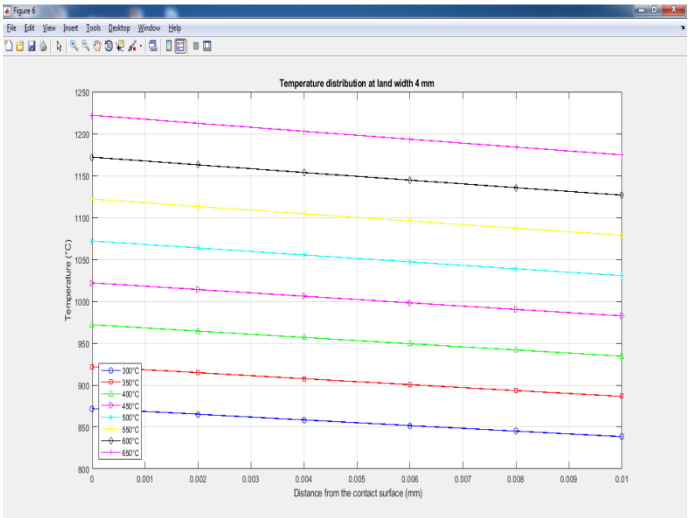

Figure 11: Temperature distribution at land width 4 mm

Hardness Distribution analysis

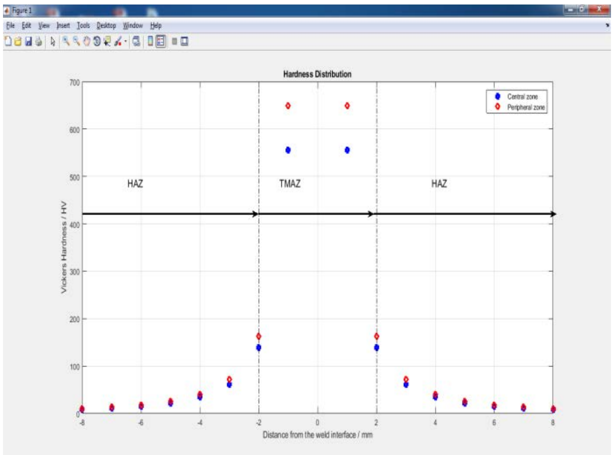

Figure 12: Hardness Distribution

Ultimate Tensile Strength (UTS) of Friction Plug Welding

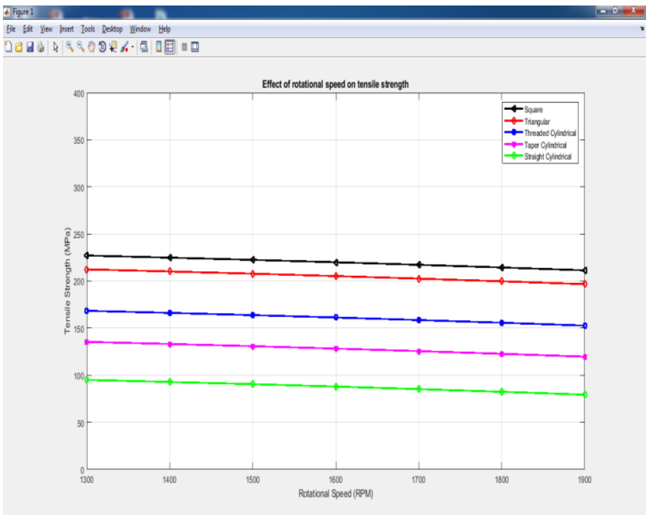

Figure 13: Effect of rotational speed on tensile strength

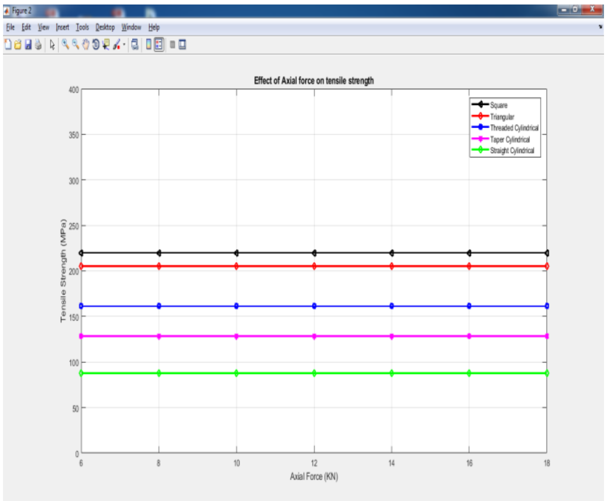

Figure 14: Effect of Axial force on tensile strength

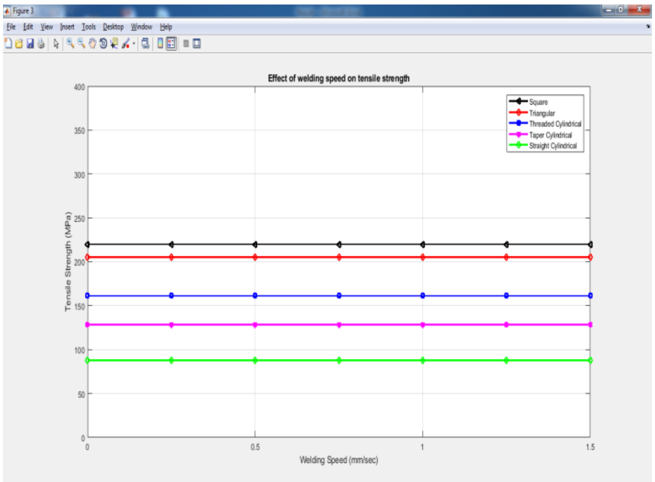

Figure 15: Effect of Welding Speed on tensile strength

V. CONCUSLION

Through the use of statistical methods such as design of experiments and regression analysis, a mathematical relationship has been constructed to predict the tensile strength of friction stir welded aluminium alloy joints by considering welding parameters and tool profiles. The calculation of the creation of heat flux due to friction between the materials takes into account the coefficient of friction. The effect of pre-heating was calculated using an analytical model. It was possible to compute the temperature distribution in the work piece for different plug diameters and varied pre-heating temperatures ranging from 250oC to 550oC using the software.

The many forms of backing materials were used in order to discover a method of controlling the microstructure and mechanical properties of aluminium alloy joints, such as hardness distribution and tensile qualities, among other things.

It has been possible to develop a mathematical relationship to predict the tensile strength of friction stir-welded aluminium alloy joints by incorporating welding parameters and tool profiles, and by employing statistical tools such as design of experiments, analysis of variance, and regression analysis.

REFERENCES

[1] Yong-Jai Kwon, Seong-Beom Shim, Dong-Hwan Park, Friction stir welding of 5052 aluminum alloy plates, Trans. Nonferrous Met. Soc. China 19(2009) s23−s27.

[2] G.Cao, S.Kou, friction stir welding of 2219 aluminum: behavior of theta (Al2Cu) particles, The Welding Journal, January 2005.

[3] J. Adamowski , C. Gambaro, E. Lertora, M. Ponte, M. Szkodo, analysis of FSW welds made of Aluminium alloy AW 6082-T6, Archives of Materials Science and Engineering, Volume 28,Issue 8,August 2007.

[4] H. J. LIU, H. FUJII, K. NOGI, Friction stir welding characteristics of 2017-T351 aluminum alloy sheet, JOURNAL OF MATERIALS SCIENCE 40 (2005) 3297 – 3299.

[5] M. Vural, A. Ogur, G. Cam, C. Ozarpa, On the friction stir welding of Aluminium alloys EN AW 2024-0 and EN AW 5754-H22, Archives of Materials Science and Engineering, Volume 28,Issue 1,January 2007.

[6] R. Nandan,T. DebRoy,H.K.D.H.Bhadeshia;Recent Advances in Friction Stir Welding – Process, Weldment Structure and Properties, Progress in Materials Science 53 (2008) 980-1023.

[7] D. M. Rodrigues, C. Leita˜o, R. Louro, H. Gouveia and A. Loureiro, High speed friction stir welding of Aluminium alloys, Science and Technology of Welding and Joining, 2010.

[8] Adler, Yu, P, Markov, E & Granovsky, YV 1975, The Design of Experiments to Find Optimal Conditions, 1st edition. Moscow, Mir publishers.

[9] Hattingh D, Doubell P, Newby M, Wedderburn I, Steuwer A and James M (2009) Friction taper stud welding of creep resistant 10CrMo910 steel, TMS, Annual Meeting & Exhibition; Friction Stir Welding and Processing-V, San Francisco, California, pp 75-84.

[10] P. Hartley, Friction plug weld repair for the space shuttle external tank, NASA document ID 20000093962, Johnson Space Center, Marshall Space Flight Center, 2000.

[11] Xuefeng Lei, Ying Deng, Zhimin Yin, nd Guofu Xu.Tungsten inert gas and friction stir welding characteristics of 4-mm-Thick 2219-T87 plates at room temperature and −196 °C 23, ASM International (2014), pp. 2149-2158.

[12] Dongun Kim, Harsha Badarinarayan, Ill Ryu1, Ji Hoon Kim, Chongmin Kim, Kazutaka Okamoto, R. H. Wagoner, Kwansoo Chung(2009), Numerical simulation of friction stir welding process, Int J Mater Form, Vol.2, pp 383-386

[13] Rosenthal, D. (1941), Mathematical theory of heat distribution during welding and cut-ting, Welding Journal20 (5), pp. 220-234.

[14] Riki Takeshita, Terry L., Kenner, Friction Plug Welding. United States Patent, Patent No:US6213379 BI, April 10, 2001.

[15] Yuh J. Chao, Shu Liu and Chi-Hui Chien (2008) friction stir welding of al 6061-t6 thick plates: part ii – numerical modeling of the thermal and heat transfer phenomena Journal of the Chinese Institute of Engineers., Vol 31, pp 769-779

[16] N. Rajesh Jesudoss Hynes, P. Nagaraj and J. Angela Jennifa Sujana, Investigation on Joining of Aluminum and Mild Steel by Friction Stud Welding, Materials and Manufacturing Processes. 27 (2012) 1409-1413.

[17] N. Rajesh Jesudoss Hynes, P. Nagaraj, R. Palanichamy, C. A. K. Arumugham and J. Angela Jennifa Sujana, Numerical Simulation of Heat Flow in Friction Stud Welding of Dissimilar Metals, Arabian Journal for Science and Engineering, DOI 10.1007/s13369-013-0932-3.

[18] N. Rajesh Jesudoss Hynes, P. Nagaraj and J. Angela Jennifa Sujana, Mechanical Evaluation and Microstructure of Friction Stud Welded Aluminium–Mild steel Joints, Arabian Journal for Science and Engineering, DOI 10.1007/s13369-014-1082-y.

[19] N. Rajesh Jesudoss Hynes, P. Nagaraj and R. Meby Selvaraj, Finite element based thermal modelling of friction welding of dissimilar materials, International Journal of Modern Physics. 22 (2013) 196–202.

[20] Mumin, S.; Erol, A.H.; Kaan, O.: An experimental study on joining of severe plastic deformed aluminium materials with friction welding method. Mater. Des. 29(1), 1–10 (2006)

[21] Ting-Fai, K.; Luen-Chow, C.; Tai-Chiu, L.:Weld diffusion analysis of forming bimetallic components using statistical experimental methods. Mater. Manufac. Processes 24(4), 422–430 (2009)

[22] Sahin, M.: Joining of stainless-steel and luminium materials by friction welding. Int. J. Adv. Manuf. Technol. 41, 487–97 (2008)

[23] Davari, H.; Parsa, M.H.; Hadian, A.M.; Nili, M.: Ahmadabadi, experimental and numerical thermomechanical analysis of hybrid friction welding of commercially pure copper bars. Mater. Manuf. Processes 26(5), 694–702 (2011)

[24] Ozdemir, N.: Investigation of themechanical properties of frictionwelded joints between AISI 304L, AISI Steel as a function rotational speed. Mater. Lett. 59, 2504–2509 (2005)

[25] R. Hancock, Friction welding of aluminum cuts energy Cost by 99%, Weld. J., 83 (2004) 40-45.

[26] L. Y. Wei and T. W. Nelson, Correlation of microstructures and process variables in FSW HSLA-65 steel, Weld. J., 90 (2011) 95s-101s.

[27] Y. Tsunekawa, H. Suzuki and Y. Genma, Application of ultrasonic vibration to in situ MMC process by electromagnetic melt stirring, Mater. Des., 22 (2001) 467-472.

[28] Y. Yang, J. Lan and X. Li, Study on bulk aluminum matrix nano-composite fabricated by ultra sonic dispersion of nanosized SiC particles in molten aluminum alloy, Mater. Sci. Eng. A, 380 (2004) 378-383.

[29] R. George, K. T. Kashyap, R. Rahul and S. Yamdagni, Strengthening in carbon nanotube/aluminum (CNT/Al) composites, Scr. Mater., 53 (2005) 1159-1163.

[30] R. Zhong, H. Cong and P. Hou, Fabrication of nano-Al based composites reinforced by single-walled carbon nanotubes, Carbon, 41 (2003) 848-851.